

Fig. S1. Embryonic and larval expression of CAP protein. (A) Stage 16 embryos were immunostained with anti-CAP and anti-MHC. CAP is present at scolopale cells (thick arrows) and muscle attachment sites (MASs) of longitudinal muscles (thin arrows) but is missing from lateral transverse muscles (arrowheads). (B) Expression pattern of CAP-GFP in the *GFP-CAP trap* line *CAPCA06924*, which harbors a GFP trap in a *CAP* intron. CAP-GFP localizes to scolopale cells (arrowheads) and MASs (arrow) in stage 16-17 embryos. (C) Wild-type and *GFP-CAP trap* larval fillets were stained with indicated antibodies. CAP colocalizes at Z-disks with Zasp. Scale bars: 5 μ m in A; 10 μ m in B; 60 μ m in C.

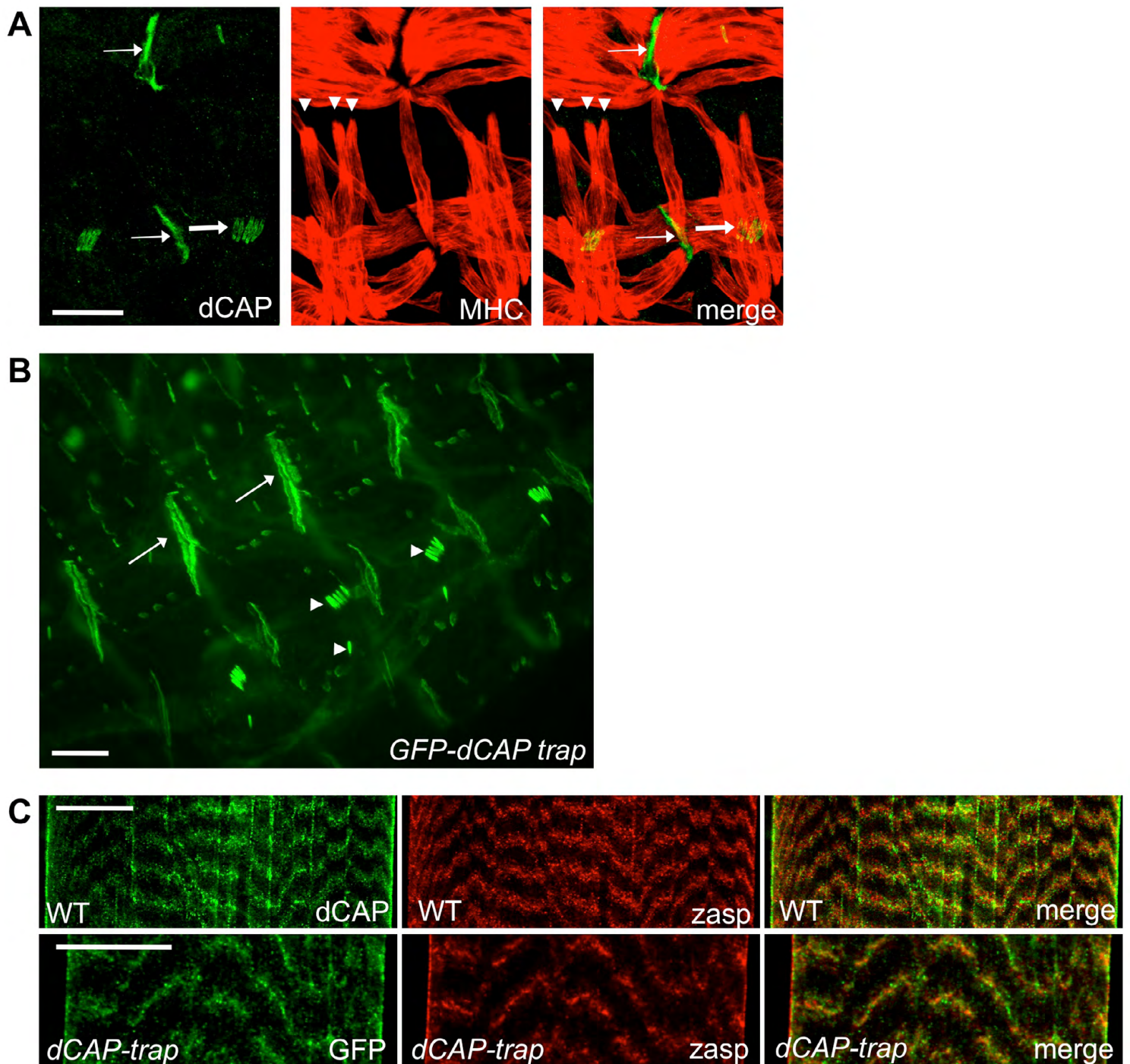


Fig. S1. Embryonic and larval expression of CAP protein. (A) Stage 16 embryos were immunostained with anti-CAP and anti-MHC. CAP is present at scolopale cells (thick arrows) and muscle attachment sites (MASs) of longitudinal muscles (thin arrows) but is missing from lateral transverse muscles (arrowheads). (B) Expression pattern of CAP-GFP in the *GFP-CAP trap* line *CAPCA06924*, which harbors a GFP trap in a *CAP* intron. CAP-GFP localizes to scolopale cells (arrowheads) and MASs (arrow) in stage 16-17 embryos. (C) Wild-type and *GFP-CAP trap* larval fillets were stained with indicated antibodies. CAP colocalizes at Z-disks with Zasp. Scale bars: 5 μ m in A; 10 μ m in B; 60 μ m in C.

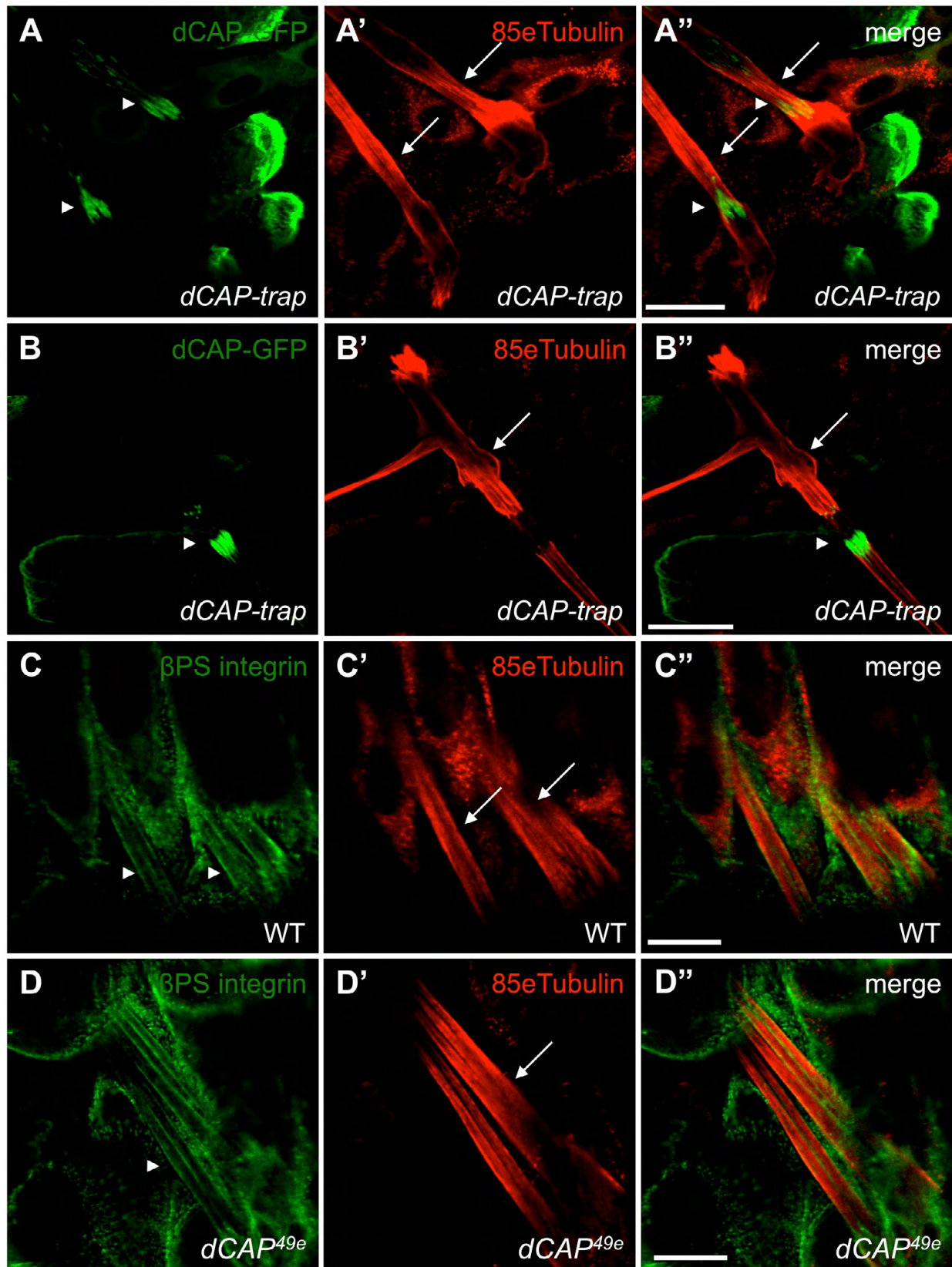


Fig. S2. Cap cells are unaffected in $dCAP^{49e}$ mutants. (A-B'') Fillet preparations from *GFP-CAP trap* animals were stained with GFP and 85e-tubulin antibodies. 85e-tubulin antibody labels cap, cap attachment cells (arrows in A' and A''), ligament cells and ligament attachment cells (arrows in B' and B''). CAP-GFP is enriched at the junction of cap and cap-attachment cells (arrowheads in A) and in scolopale cells (arrowhead in B). (C-D'') Wild-type and $dCAP^{49e}$ larval fillet preparations were stained with β PS integrin (arrowheads) and 85e-tubulin antibody (arrows). β PS integrin localization in cap cells is unaltered in *CAP* mutants. Scale bars: 40 μ m in A-B''; 20 μ m in C-D''.

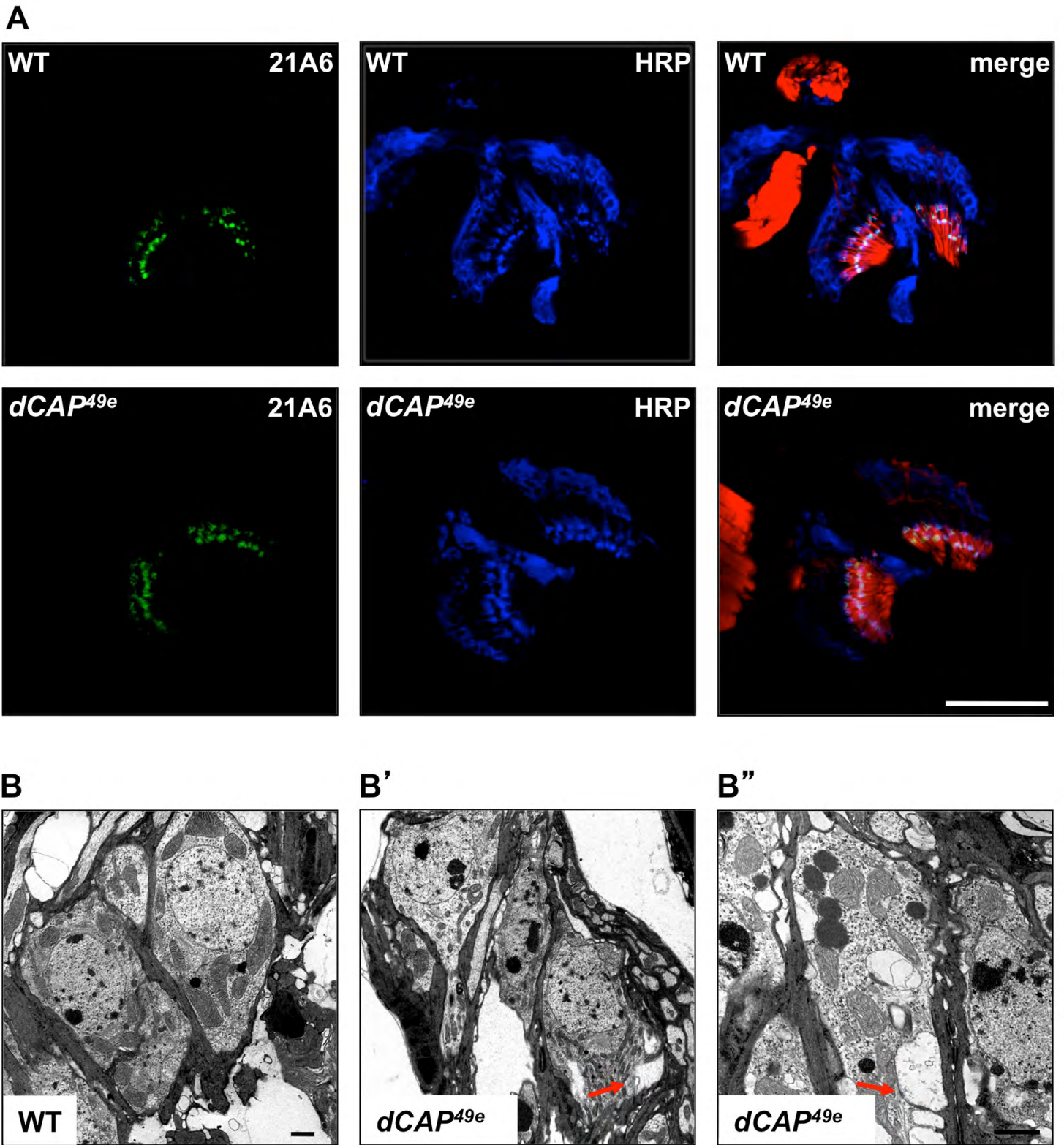


Fig. S3. Morphological analysis of Johnston's organs in *dCAP^{49e}* mutants. (A) Sections of Johnston's organ from wild-type and *dCAP^{49e}* adult flies were stained with phalloidin, MAb 21A6 and HRP (which labels neurons). No defects were observed in the 21A6 staining in *CAP* mutants. (B) TEM images of wild-type and *dCAP^{49e}* Johnston's organ sections, showing neurons with abnormal vacuolar structure (arrows) in *dCAP^{49e}* mutants. Scale bars: 30 μm in A; 1 μm in B.

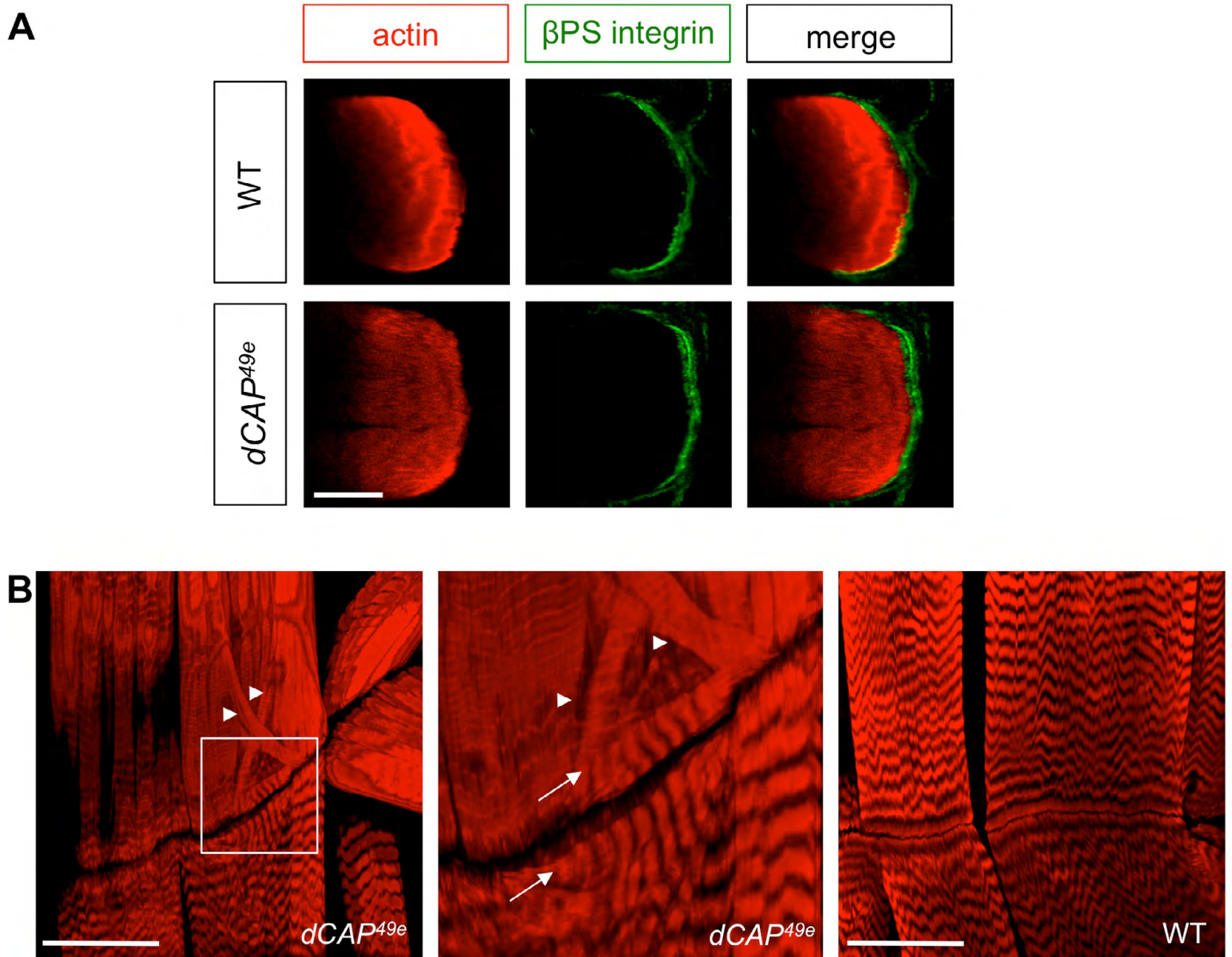


Fig. S4. Morphological analysis of MASS in *dCAP^{49e}* mutants. (A) Lateral transverse muscles of wild-type and *dCAP^{49e}* mutant larvae were immunostained with phalloidin and β PS integrin antibody. (B) Muscle attachment sites of *dCAP^{49e}* larvae often show an aberrant morphology (arrows), with myofilaments organized in a perpendicular orientation relative to wild-type animals and disorganization of myofilaments near the sarcolemma (arrowheads). Middle panel shows magnified image of inset. Scale bars: 20 μ m in A; 60 μ m in B.

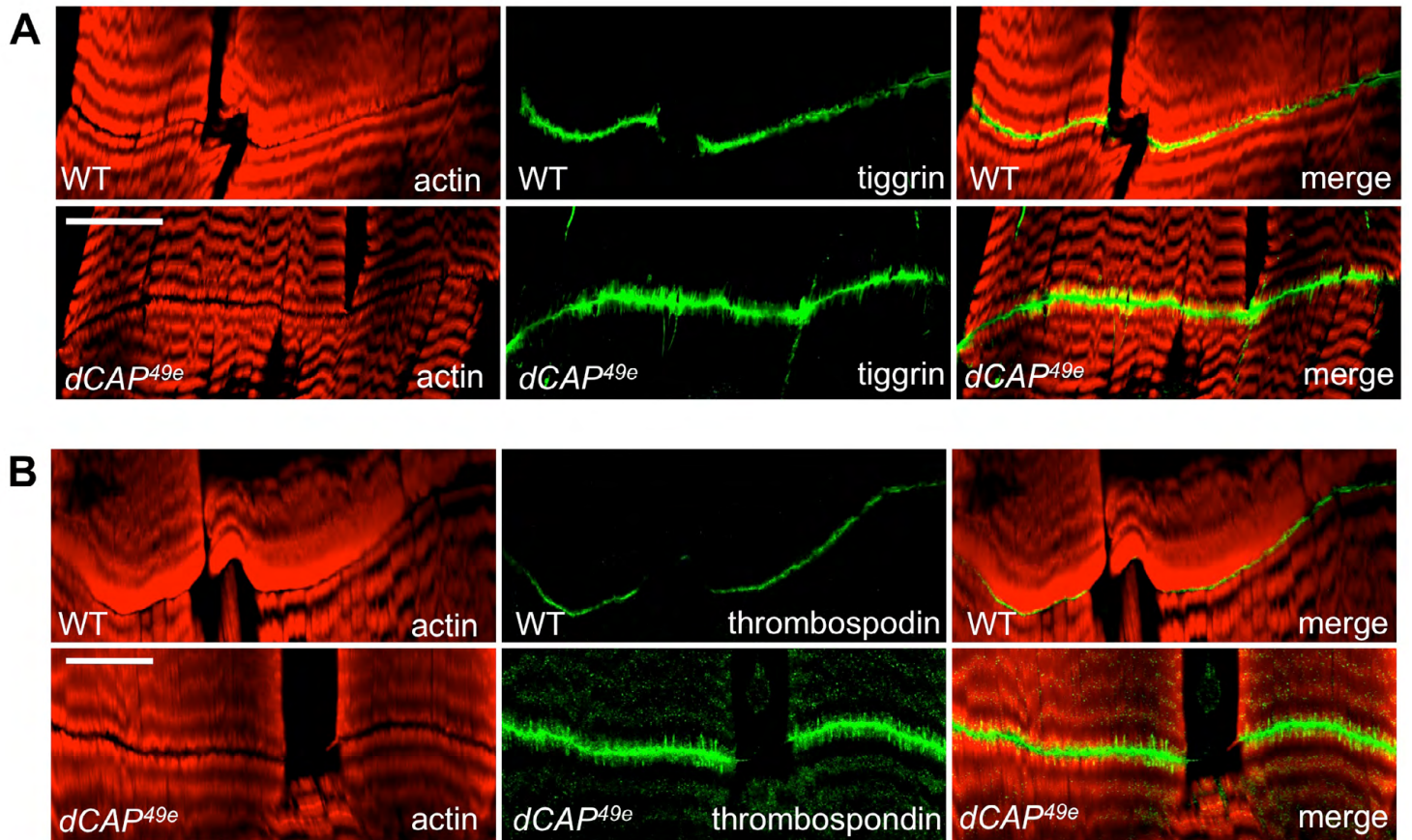


Fig. S5. Tigrin and Thrombospondin show altered distribution in *dCAP^{49e}* mutants. (A) Wild-type and *dCAP^{49e}* larvae were stained with anti-Tigrin and phalloidin. (B) Wild-type and *dCAP^{49e}* larvae were stained with anti-thrombospondin and phalloidin. Scale bars: 30 μm .

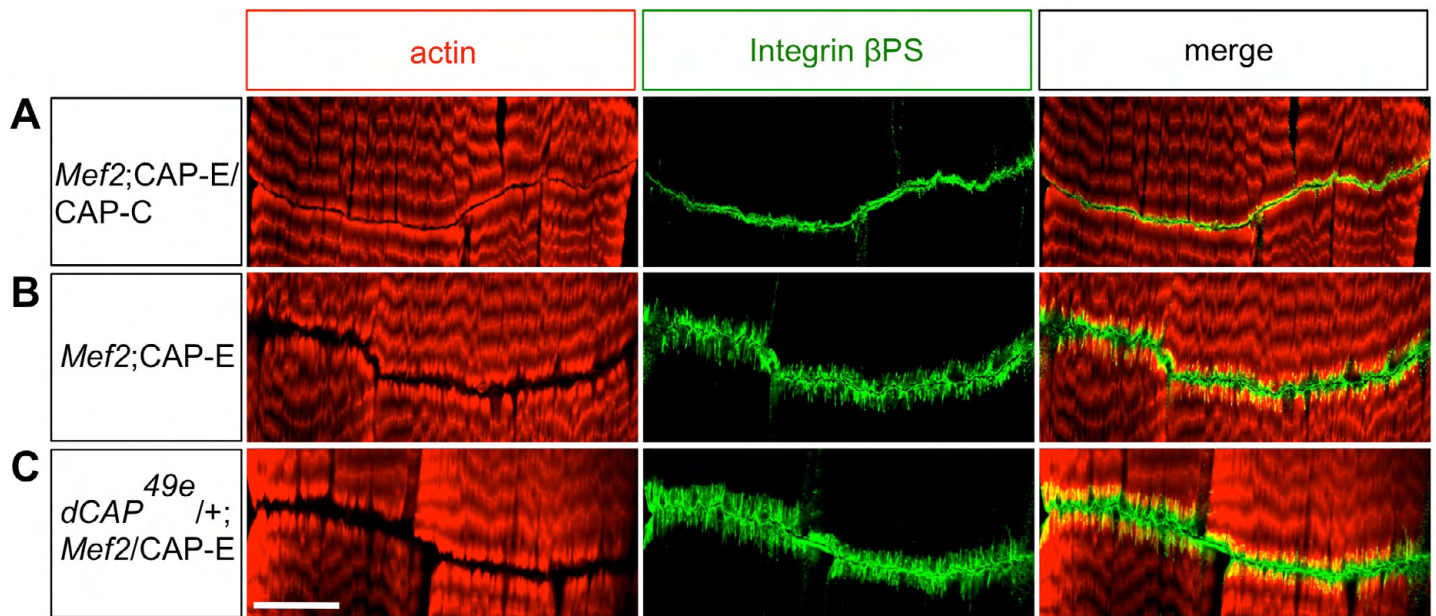


Fig. S6. Co-expression of dCAP-C suppresses dCAP-E GOF defects. *Mef2-Gal4* was used to overexpress dCAP isoforms in muscles. (A) dCAP-E and dCAP-C were co-expressed in muscles. (B) Only the dCAP-E isoform was expressed in muscles. (C) dCAP-E was overexpressed in a *dCAP*^{49e} heterozygous background. Scale bars: 30 μ m in A-C.

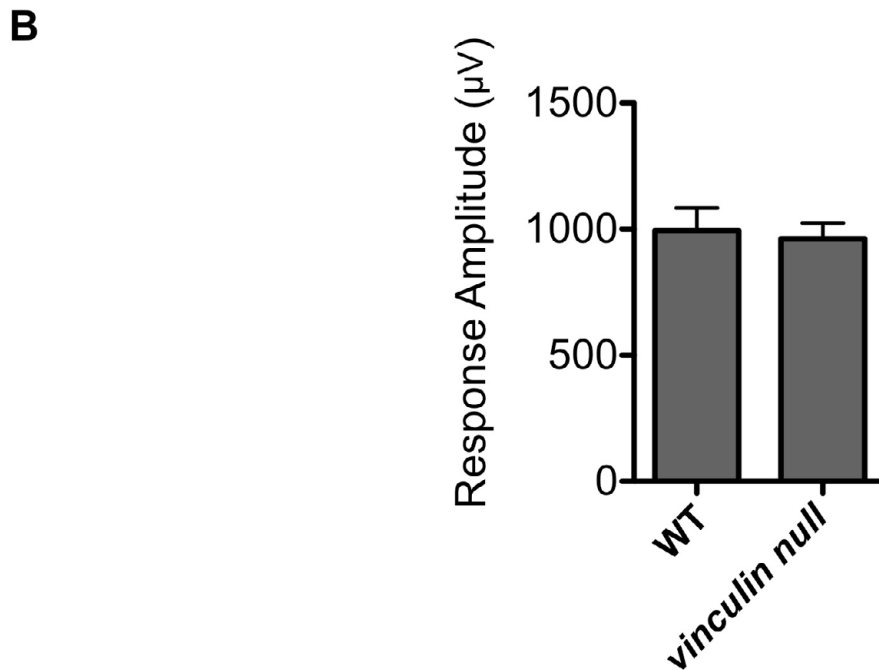
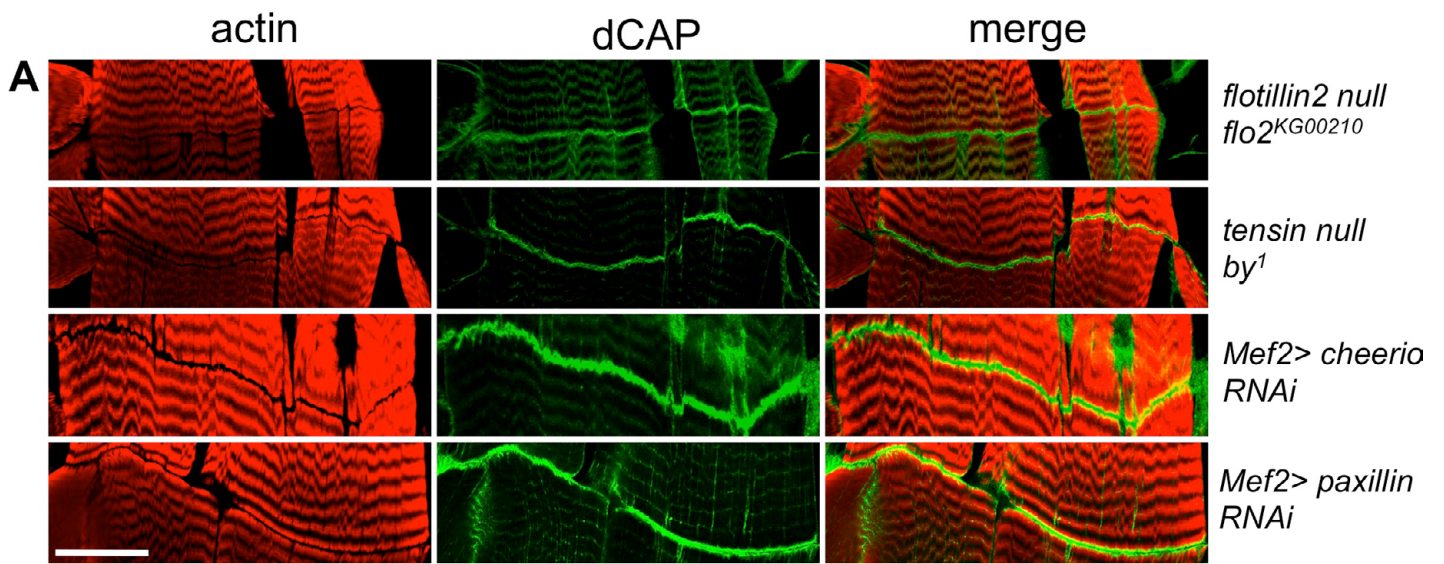


Fig. S7. MAS and audition analysis in animals lacking CAP-binding proteins. (A) Muscle attachment sites of larval fillets from indicated genotypes were labeled with phalloidin and CAP antibody. No abnormalities were detected in *tensin*- and *flotillin*-null larvae, or in larvae expressing *cheerio* (*filamin*) or *paxillin* RNAi under the *Mef2-Gal4* driver. Scale bars: 30 µm. (B) Sound-evoked potentials recorded from the auditory nerves of wild type and *vinculin*-null flies ($n=10$ animals).

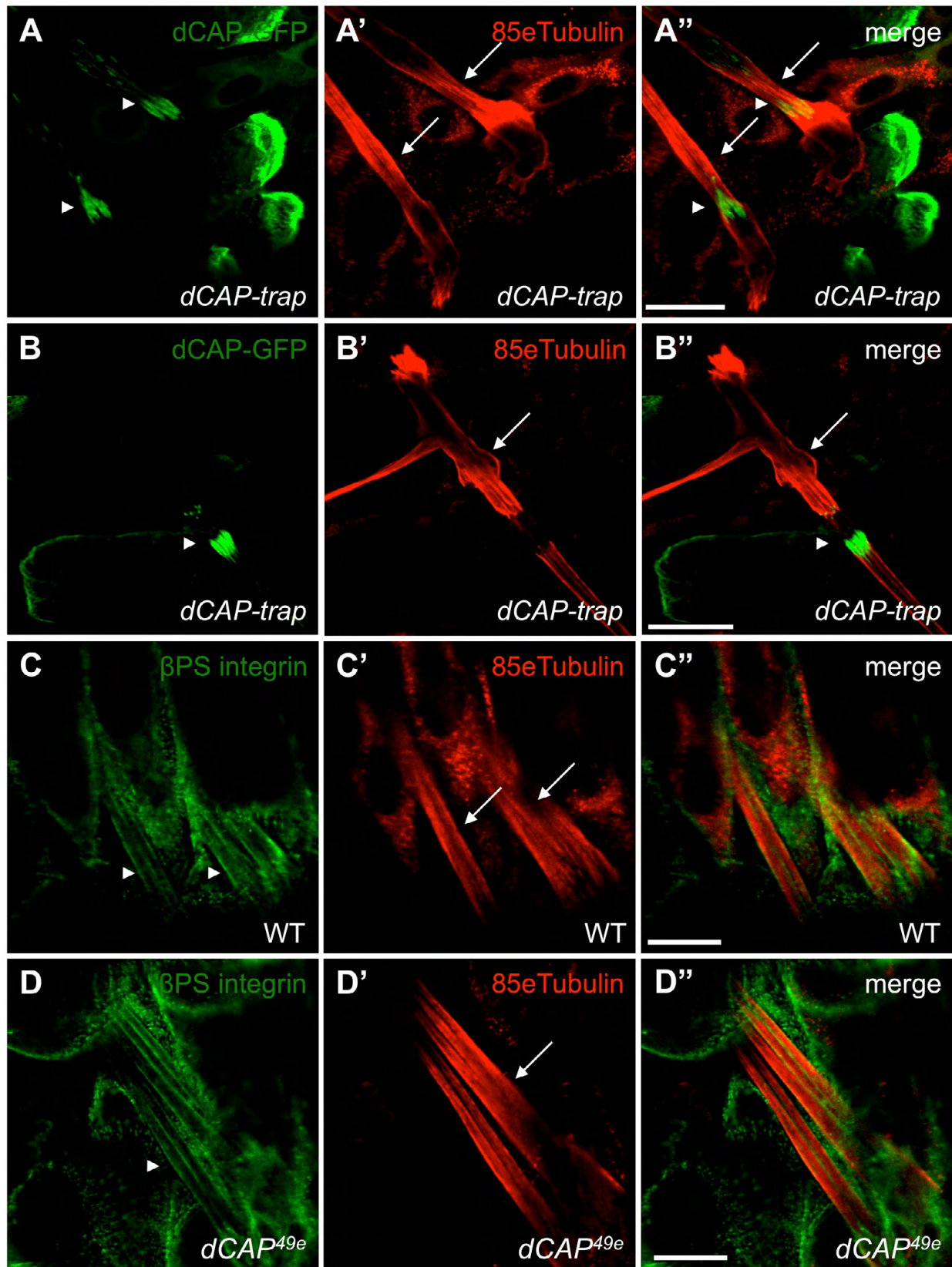


Fig. S2. Cap cells are unaffected in *dCAP^{49e}* mutants. (A-B'') Fillet preparations from *GFP-CAP trap* animals were stained with GFP and 85e-tubulin antibodies. 85e-tubulin antibody labels cap, cap attachment cells (arrows in A' and A''), ligament cells and ligament attachment cells (arrows in B' and B''). CAP-GFP is enriched at the junction of cap and cap-attachment cells (arrowheads in A) and in scolopale cells (arrowhead in B). (C-D'') Wild-type and *dCAP^{49e}* larval fillet preparations were stained with β PS integrin (arrowheads) and 85e-tubulin antibody (arrows). β PS integrin localization in cap cells is unaltered in *CAP* mutants. Scale bars: 40 μ m in A-B''; 20 μ m in C-D''.

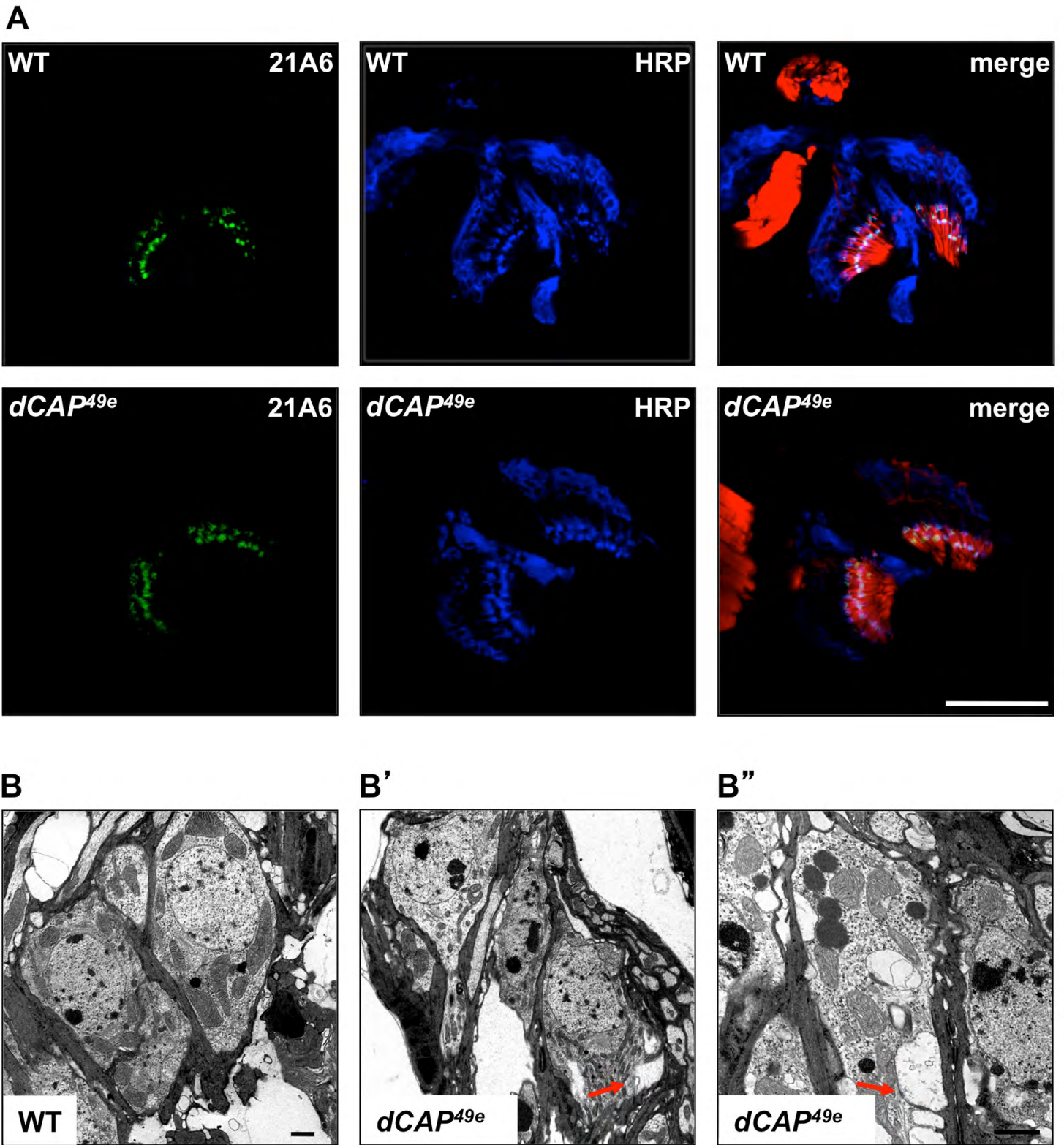


Fig. S3. Morphological analysis of Johnston's organs in *dCAP^{49e}* mutants. (A) Sections of Johnston's organ from wild-type and *dCAP^{49e}* adult flies were stained with phalloidin, MAb 21A6 and HRP (which labels neurons). No defects were observed in the 21A6 staining in *CAP* mutants. (B) TEM images of wild-type and *dCAP^{49e}* Johnston's organ sections, showing neurons with abnormal vacuolar structure (arrows) in *dCAP^{49e}* mutants. Scale bars: 30 μm in A; 1 μm in B.

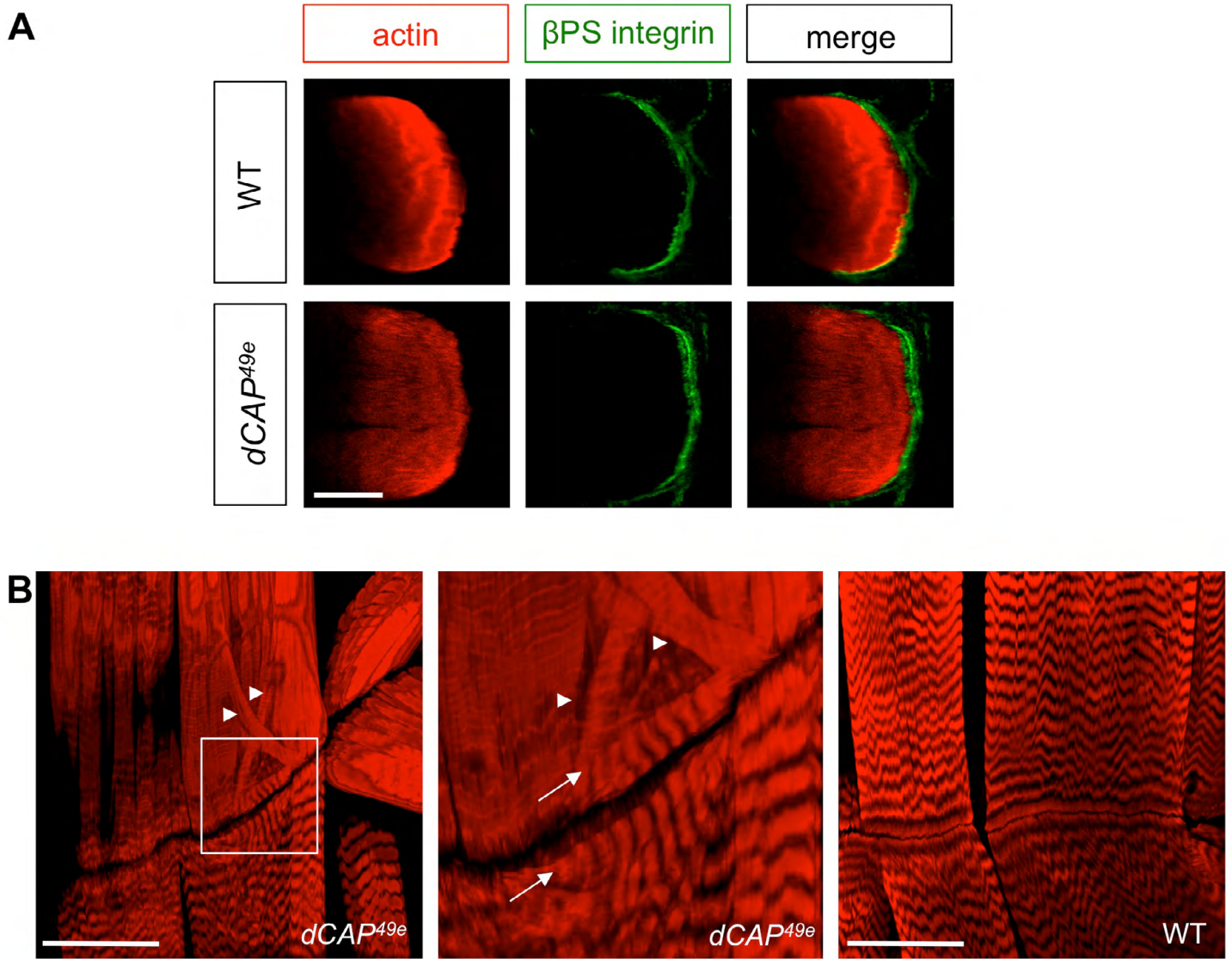


Fig. S4. Morphological analysis of MASS in *dCAP^{49e}* mutants. (A) Lateral transverse muscles of wild-type and *dCAP^{49e}* mutant larvae were immunostained with phalloidin and β PS integrin antibody. (B) Muscle attachment sites of *dCAP^{49e}* larvae often show an aberrant morphology (arrows), with myofilaments organized in a perpendicular orientation relative to wild-type animals and disorganization of myofilaments near the sarcolemma (arrowheads). Middle panel shows magnified image of inset. Scale bars: 20 μ m in A; 60 μ m in B.

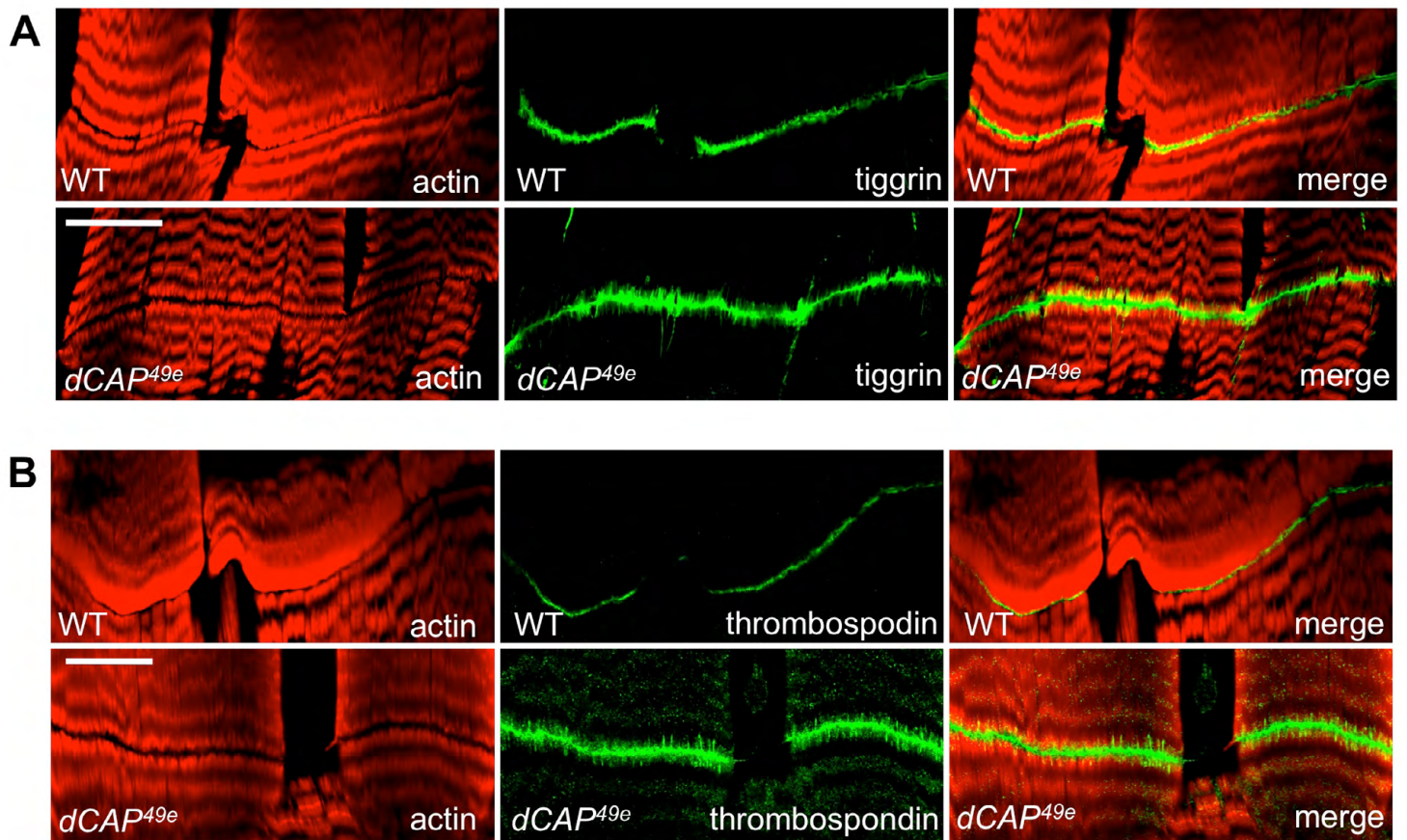


Fig. S5. Tiggrin and Thrombospondin show altered distribution in *dCAP^{49e}* mutants. (A) Wild-type and *dCAP^{49e}* larvae were stained with anti-Tiggrin and phalloidin. (B) Wild-type and *dCAP^{49e}* larvae were stained with anti-thrombospondin and phalloidin. Scale bars: 30 μm .

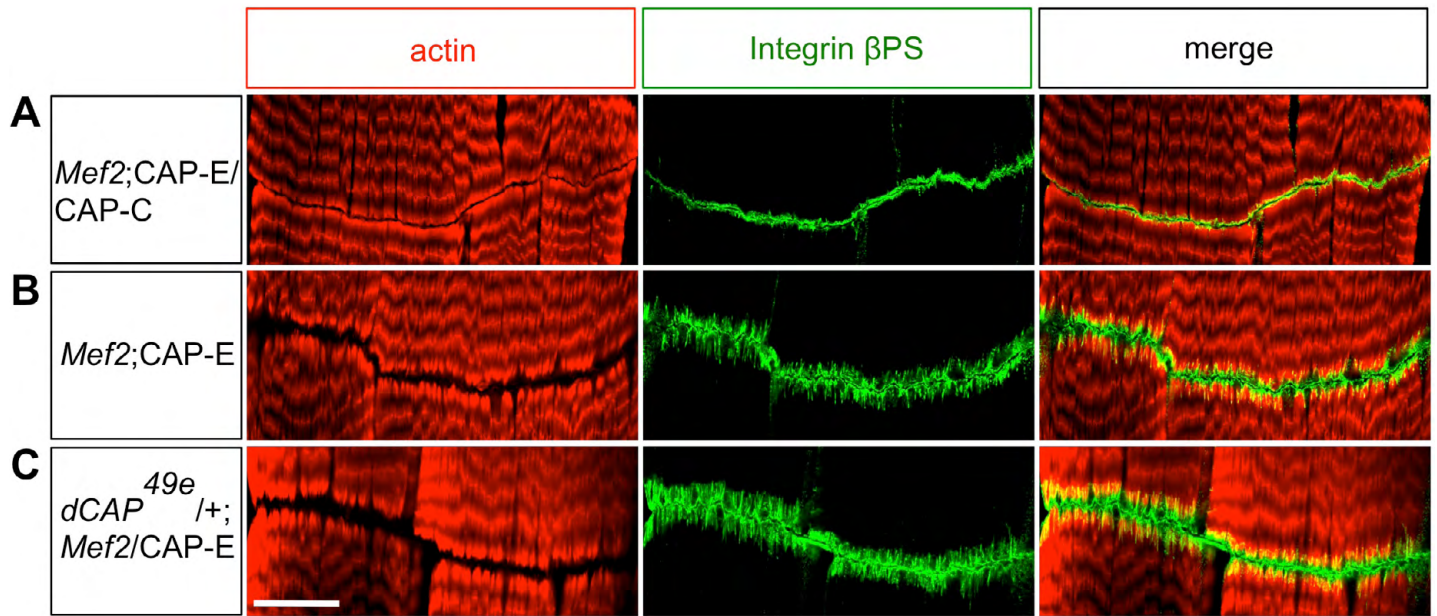


Fig. S6. Co-expression of dCAP-C suppresses dCAP-E GOF defects. *Mef2-Gal4* was used to overexpress dCAP isoforms in muscles. (A) dCAP-E and dCAP-C were co-expressed in muscles. (B) Only the dCAP-E isoform was expressed in muscles. (C) dCAP-E was overexpressed in a *dCAP*^{49e} heterozygous background. Scale bars: 30 μ m in A-C.

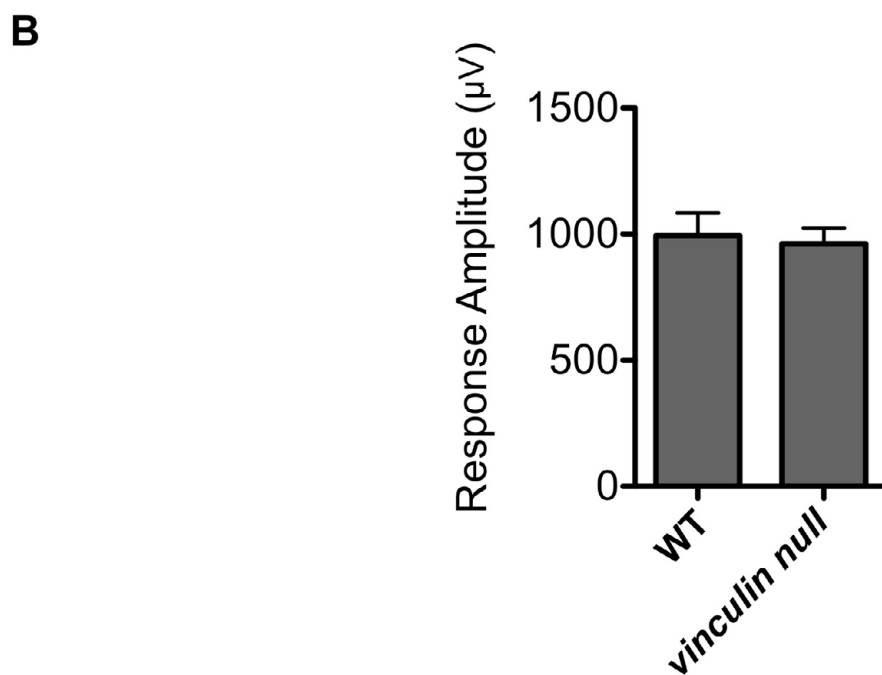
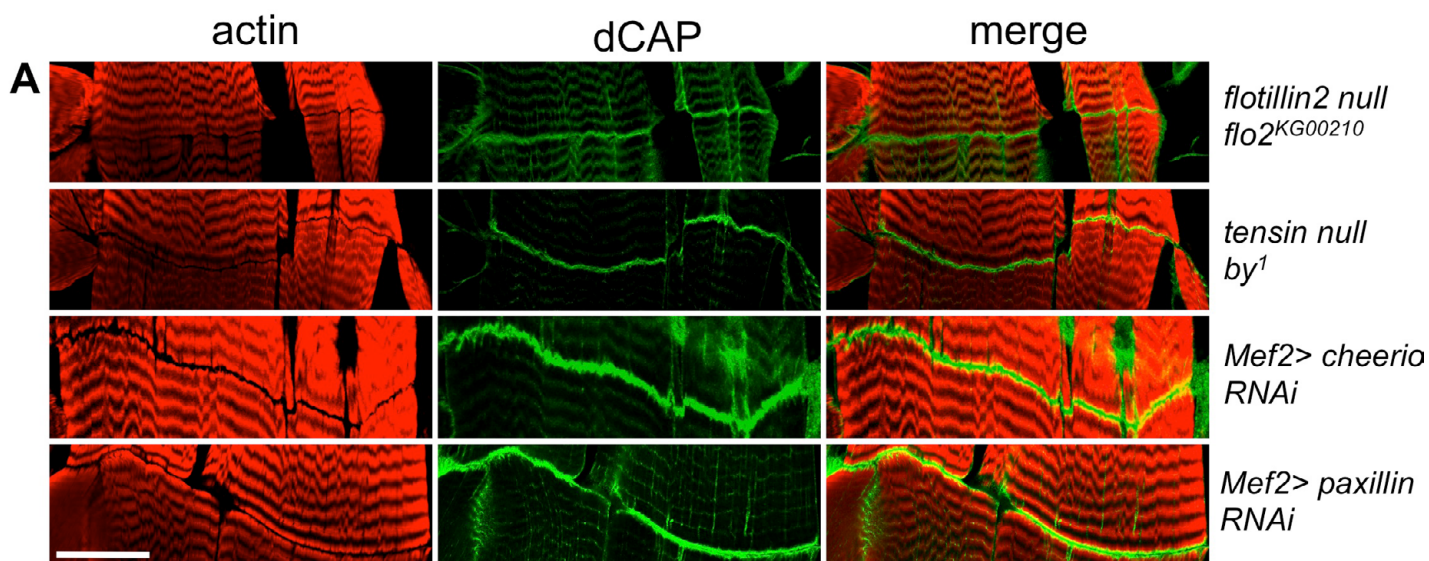


Fig. S7. MAS and audition analysis in animals lacking CAP-binding proteins. (A) Muscle attachment sites of larval fillets from indicated genotypes were labeled with phalloidin and CAP antibody. No abnormalities were detected in *tensin*- and *flotillin*-null larvae, or in larvae expressing *cheerio* (*filamin*) or *paxillin* RNAi under the *Mef2-Gal4* driver. Scale bars: 30 µm. (B) Sound-evoked potentials recorded from the auditory nerves of wild type and *vinculin*-null flies ($n=10$ animals).